RELATIONSHIPS BETWEEN FATIGUE CRACK GROWTH AND ACOUSTIC EMISSION IN CMn STRUCTURAL STEEL

C. Thaulow and M. Hval

The Foundation of Scientific and Industrial Research at the Norwegian Institute of Technology, SINTEF, N-7034 Trondheim, NTH, Norway

ABSTRACT

Primary acoustic emission (AE) signals from fatigue crack growth in structural CMn steel, have been recorded and compared with fracture mechanics parameters.

Two samples were tested, with crack growing in the ST and LS orientation.

Several correlations were established between the AE and the fracture mechanics parameters. The best fit to linear regression analysis was obtained for correlations of the form

$$\dot{N} \sim \dot{a}\, K_{max}^{6}/(K_C - K_{max})$$

KEYWORDS

Acoustic emission, fracture mechanics, fatigue, correlation analysis.

LIST OF SYMBOLS

$\dot{a}$	fatigue crack growth per load cycle
a	crack length
Δa	crack growth distance
C,p,q,m,n	constants
K_{max}	maximum stress intensity factor
K_C	fracture toughness
ΔK	$K_{max} - K_{min}$
R	K_{min}/K_{max}
N_e	acoustic emission event
$\dot{N}_e$	acoustic emission event per load cycle
N	acoustic emission count
$\dot{N}$	acoustic emission counts per load cycle
B	specimen thickness
E	modulus of elasticity

σ_y yield stress
Δn number of load cycles

INTRODUCTION

The acoustic emission sources generated during fatigue - and corrosion fatigue crack growth can be separated in primary and secondary sources.

A large research programme has been carried out in order to determine the characteristics of AE from corrosion fatigue crack growth and evaluate the application of AE monitoring of offshore structures.

The main AE sources from corrosion fatigue cracks are secondary emissions generated by interaction of corrosion products, but under certain circumstances primary emissions might be important and the present experiments have been performed in order to examine the primary AE activity during fatigue loading of a BS 4360 grade 50D structural steel.

During the research programme the following characteristics for the primary AE have been established:

1) The amplitudes are usually lower than 50 - 60 dB.
2) The activity is distributed over the whole crack growth monitoring period.
3) The signals are recorded on rising load, eg. when the crack is opening, close to max load in the fatigue cycle.

These criteria have been used in the present experiments in order to separate the primary and secondary emissions.

Theoretical evaluations and experimental investigations have verified that relationships can be established between primary AE and fracture mechanics parameters. [1, 2, 3].

EXPERIMENTAL

Test Set Up

Two single edge notch specimens, Fig. 1, of a BS 4360 Grade 50D steel (0.17 % C, 1.30 % Mn, 0.40 % Si), with two different orientations of the crack plane (L-S and S-T) have been tested in 4 point bending fatigue, Fig. 1.

The crack depth was measured with a special developed DC potential drop instrumentation, with a resolution of 0.02 - 0.05 mm.

AE Instrumentation

6 channels were used, Fig. 2. 2 transducers were positioned 6 cm at each side of the notch and four guard transducers were placed near each load point to pick up possible noise.

The signals were recorded and analysed with a Dunegan/Endevco 1032D system with D/E D9203A 200 kHz resonant transducers.

Test Parameters

The specimens were loaded in air fatigue with a load frequency of 1 Hz, R-ratios of 0.1, 0.33 and 0.5, and stress intensity factors ranging from 20-86 MPa $m^{\frac{1}{2}}$.

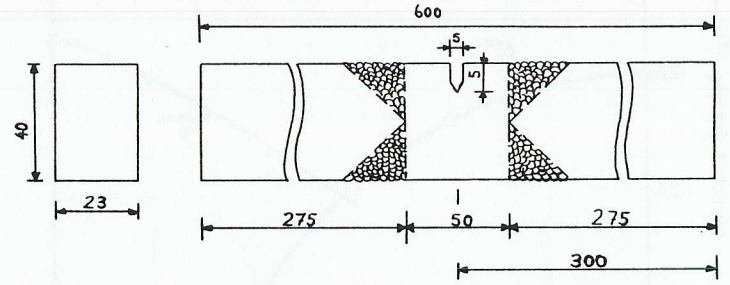

Fig. 1 Dimensions of the test specimen. The weld is only for specimen ST. All dimensions in mm.

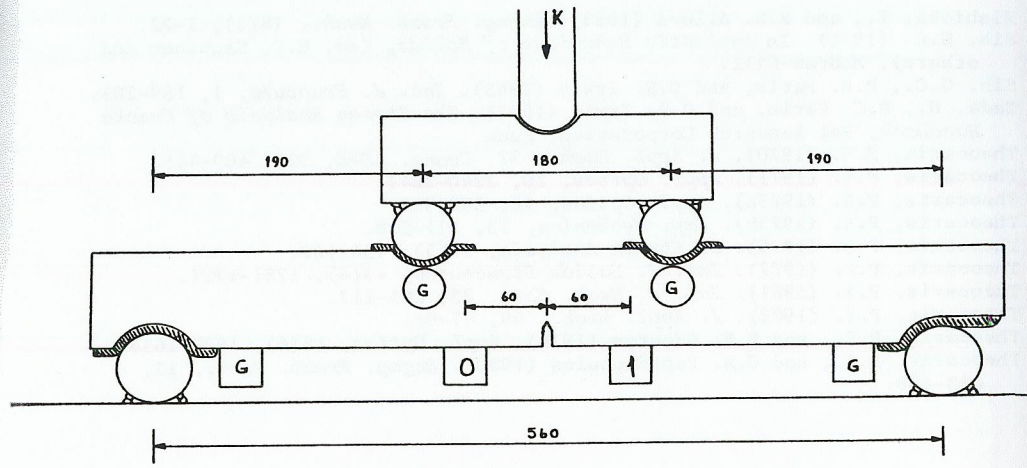

Fig. 2 Four point bending test set up. The position of the six AE transducers are indicated. Leather is glued to each load point in order to eliminate noise from the fixture and actuator. All dimensions in mm.

RESULTS

Test Specimen LS

AE activity near max load could be observed almost from the beginning of crack growth and during each increase in max load.

The AE count rate ranged from 0.06 - 1.6 counts per cycle.

Test Specimen ST

The AE activity was higher than observed in the LS test. Towards the end of the test very high crack growth rates were recorded, and the critical stress intensity factor K_C, was assumed to be in the range of 75 - 85 MPam$^{\frac{1}{2}}$. The count rate ranged from 0.02 to 6000 counts per fatigue cycle.

The Amplitude Distribution

One major slope was observed for the cumulative amplitude distribution, Fig. 3, with slopes in the range of 2.5 - 3.5.

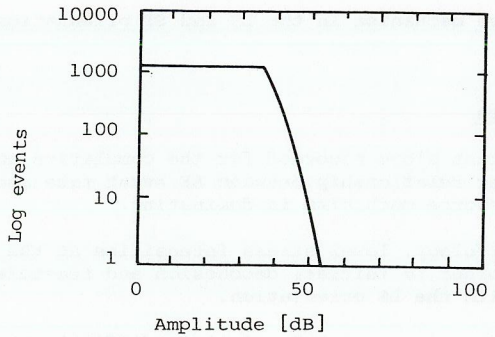

Fig.3 Typical example of the cumulative amplitude distributions recorded.

Correlation Analysis

Correlation parameters

In order to establish correlations between the AE parameters and the fracture mechanics parameters, a simple software programme was developed for the HP 85 desk computer. Nine parameters were selected as candidates for the correlation analysis: R, Δa, $\dot{a}$, a, K_{max}, ΔK, $\dot{N}e$, $\dot{N}$, Δn.

Each test (LS and ST) was divided in several sets, and the parameters from each set were input to the computer analysis. A typical analysis could be correlations of the form:

$$\dot{N} = C\Delta K^m$$

$$\log \dot{N} = \log C + \log \Delta K$$

Lines were fitted to the data using linear regression, with the parameters a, b and r^2. Where r^2 is the correlation coefficient.

Initially, the test specimen LS was represented with 58 sets and the test specimen ST with 99 sets. The sets represented a wide range of crack growth distances, Δa, and during the analysis it was realised that Δa for each set preferably should be in the same range. The data was then rearranged in order to keep Δa close to 1 mm as a common parameter. The number of sets was then reduced to 11 sets for LS and 14 sets for ST.

Fatigue crack growth rates

The LS-series fit very well to a Paris law relationship, Fig. 4, while the ST series have a lower correlation coefficient, $r^2 = 0.5$, due to the very high crack growth rates measured at the last stages of the test (set 24 and 25).

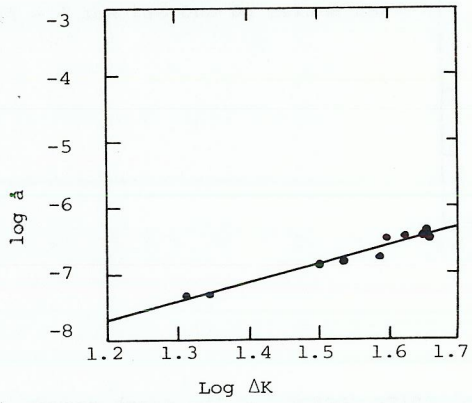

Fig. 4
Correlation between:
$\dot{a} \sim \Delta K$. Test series LS,
data set 1 - 11. $r^2 = 0.96$.

Correlation between $\dot{N}$ and ΔK

When the AE data are fitted in accordance with a similar power law as Paris law, relatively poor correlations are obtained. The ST test has the best fit, with $r^2 = 0.70$.

In order to include the effect of R-ratio and the effect of other crack growth mechanisms than striation formation (micro cleavage and intergranular failure), the parameters R and K_C have been included in the analysis of the form:

$$\dot{N} \sim \Delta K^P/(1-R)(K_C - K_{max})$$

K_C has been estimated to be 75 - 85 MPa m$^{\frac{1}{2}}$ for the ST orientation and 85 - 90 MPa m$^{\frac{1}{2}}$ for the LS orientation.

The correlations for the LS series are still poor, but a very good correlation coefficient is now obtained for the ST series, $r^2 = 0.97$ with $p = 2$ and $K_C = 75$ MPa m$^{\frac{1}{2}}$.

Correlation between $\dot{N}$ and $\dot{a}$

The LS series have a low correlation coefficient while the ST series have a good fit, with $r^2 = 0.89 - 0.92$.

The low linear regression correlation for the LS series is due to two data sets, set 3 and 4. These two sets fit very well to the regression line for the ST series, Fig. 5, and it is therefore close at hand to assume that the AE sources or source mechanisms, for set 3 and 4 are similar to those experienced in the ST series.

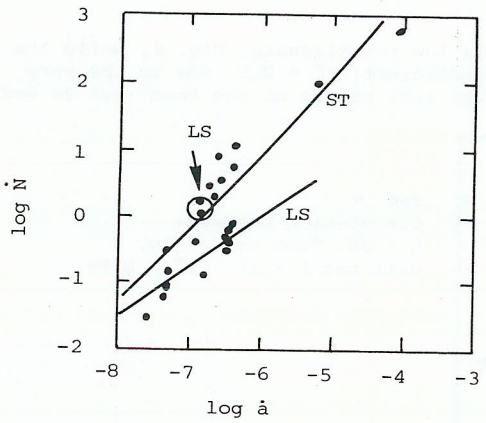

Fig. 5
Correlation between: $\dot{N} \sim \dot{a}$.
Test series LS and ST, set 1 - 25.

Correlation between $\dot{N}$ and $\dot{a}\ K_{max}^P$

In order to include both the stress intensity factor and the crack growth rate, the product of $\dot{a}$ and K_{max}^2 has been correlated with $\dot{N}$. The ST series have a very good correlation:

$$\dot{N} \simeq 3.1 \cdot 10^3\ \dot{a} \cdot K_{max}^2,\ r^2 = 0.97$$

Again set 3 and 4 from the LS series, fit into the ST-series, giving a low degree of correlation for the LS series.

In order to include the effect of the K_{max} values close to K_C, and normalize the correlation with respect to $(K_C - K_{max})$, a correlation of the form:

$$\dot{N} \sim \dot{a}\ K_{max}^P/(K_C - K_{max})$$

has been included, Fig. 6. The highest correlation coefficient was obtained for P = 6, giving $r^2 = 0.994$ and b = 0.556.

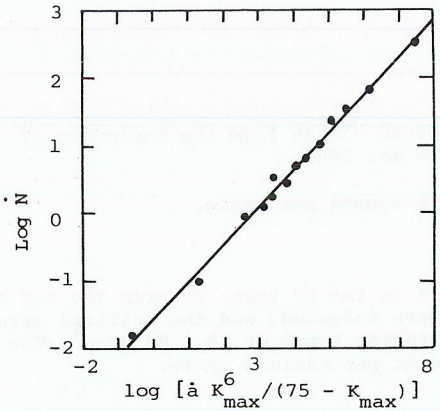

Fig. 6
Correlation between:
$\dot{N} \sim \dot{a}\ K_{max}^6/(75 - K_{max})$
Test series ST, set 12 - 25.
$r^2 = 0.994$

Correlation between AE event rate and count rate

The correlation analysis between $\dot{N}_e$ and $\dot{N}$ shows a very good fit:

$$\dot{N} \simeq 20 \cdot \dot{N}_e,\ r^2 = 0.96$$

indicating the same AE source mechanism in the LS and ST orientation.

DISCUSSION

The AE Source Characteristics

The linear, and almost constant slope recorded for the cumulative amplitude distributions, and the linear relationship between AE event rate and count rate indicates that one AE source mechanism is dominating.

Because of the inclusion morfology, lower stress intensities at the fatigue crack tip are necessary in order to initiate decohesion and fracture of the inclusions in ST compared with the LS orientation.

K_{max} and $\dot{a}$ are, to some degree, interrelated and it is difficult to determine the effect of the individual parameters. But at a certain level of stress intensity, the number of AE counts are 10 - 100 times higher in the ST orientation compared with LS. Hence the ST orientation is more favourable with respect to activate the AE sources and the activity increases as K_{max} is approaching K_C.

The most probable AE source is debonding or fracture of the sulfide inclusions. Experiments from slow bend and tensile testing of a low alloy steel, concluded that the AE source was always debonding of maganese sulfide inclusions [4].

Initial scanning electrone microscope examinations, identified fractured inclusions on the fatigue surfaces, indicating that inclusion cracking is an AE source in the present investigation. But the fracture surface examinations have been brief, and more detailed analysis should be included.

The mechanism of inclusion debonding and fracture in fatigue can not be compared directly with the deformation characteristics during tensile testing and slow bending. The next step in the examination of the primary AE sources in fatigue should include a review of possible theories for inclusion

debonding/fracture and then to correlate the AE activity with the parameters describing the inclusion debonding/fracture, such as: Inclusion morfology, volume fraction, inclusion size distribution functions, fracture mechanics parameters.

Delaminations

Specimen LS has some periods with high AE response, set 3 and 4, resulting in low correlation coefficients. Set 3 and 4 deviated in the linear regression analysis for the LS orientation, but the two sets fit to the regression line for the ST series, Fig. 6.

Scanning electrone microscope examination of the fracture surface of the LS specimen, revealed regions with delaminations perpendicular to the fracture surface, eg. in the rolling direction. The first evidences of delaminations are observed in the same area of the crack as where set 3 and 4 were recorded, and it is therefore suggested that the increased AE activity for set 3 and 4 in the LS-orientation is due to crack growth, through delaminations, in the SL (comparable with ST) orientation.

Correlation Analysis

The correlation analysis for the LS orientation was generally poor, mainly because of data set 3 and 4, see the previous section. The result of the correlations in the ST orientation is summarized in table 1.

The results indicate that equations of the form $\dot{N} \sim \dot{a}\, K_{max}^2$, give very good correlations. The correlation coefficient reached an optimum when the effect of K_{max} approaching K_C was included.

$$\dot{N} \sim \dot{a}\, K_{max}^6/(K_C - K_{max})$$

Table 1. Summary of the correlation analysis for specimen ST

Equation	Linear regression parameters	
	r^2	b
$\dot{N} \sim \Delta K$	0.69	9.16
$\dot{N} \sim \frac{\Delta K^2}{(1-R)(75-K_{max})}$	0.97	2.02
$\dot{N} \sim \dot{a}$	0.89	1.17
$\dot{N} \sim \dot{a}\, K_{max}^2$	0.97	0.96
$\dot{N} \sim \frac{\dot{a}\, K_{max}^6}{(K_C-K_{max})}$	0.99	0.556
$\dot{N} \sim \dot{a}^{K_{max}}$	0.42	-0.01

ACKNOWLEDGEMENT

The authors gratefully acknowledge the support from Norsk Hydro a.s., Conoco Norway Inc., Texaco Exploration Norway, Phillips Petroleum Company, Det norske Veritas and Safety Offshore board of Norway (SPS).

CONCLUSIONS

The primary AE source from fatigue crack growth in small scale structural steel samples has been characterized in dependence of specimen orientation.

1. The characteristics of the AE signal are similar in both ST and LS orientation.
2. The maximum AE amplitude is relatively low and do usually not exceed 50 - 60 dB.
3. The number of active sources increases with increasing stress intensity factor (and crack growth rate). The ST orientation has the highest AE activity.
4. The best fit to linear regression analysis was obtained for correlations of the form:

$$\dot{N} \sim \dot{a}\, K_{max}^6/(K_C - K_{max})$$

REFERENCES

[1] Morton, T.M., Smith, S., Harrington, R.M. (1974). Experimental Mechanics. May, pp. 208 - 213.

[2] Lindley, T.C., Palmer, I.G., Richards, C.E. (1978). Materials Science and Engineering, 32, pp. 1 - 15.

[3] Williams, J.H., Delonga, D.M., Lee, S.S. (1982), Materials Evaluation, 40, pp. 1184 - 1189.

[4] Ono, K., Yamamoto, M. (1981). Materials Science and Engineering, 47, pp. 247 - 263.